A Kriging Model for Dynamics of Mechanical Systems With Revolute Joint Clearances

Zhenhua Zhang
Department of Mechanical Engineering,
Wichita State University,
Wichita, KS 67260
e-mail: zxzhang1@wichita.edu

Liang Xu
Department of Mechanical Engineering,
Wichita State University,
Wichita, KS 67260
e-mail: lxxu3@wichita.edu

Paulo Flores
Departamento de Engenharia Mecânica,
Universidade do Minho,
Campus de Azurém,
4800-058 Guimarães, Portugal
e-mail: pflores@dem.uminho.pt

Hamid M. Lankarani
Department of Mechanical Engineering,
Wichita State University,
Wichita, KS 67260
e-mail: hamid.lankarani@wichita.edu

Over the past two decades, extensive work has been conducted on the dynamic effect of joint clearances in multibody mechanical systems. In contrast, little work has been devoted to optimizing the performance of these systems. In this study, the analysis of revolute joint clearance is formulated in terms of a Hertzian-based contact force model. For illustration, the classical slider-crank mechanism with a revolute clearance joint at the piston pin is presented and a simulation model is developed using the analysis/design software MSC.ADAMS. The clearance is modeled as a pin-in-a-hole surface-to-surface dry contact, with an appropriate contact force model between the joint and bearing surfaces. Different simulations are performed to demonstrate the influence of the joint clearance size and the input crank speed on the dynamic behavior of the system with the joint clearance. In the modeling and simulation of the experimental setup and in the followed parametric study with a slightly revised system, both the Hertzian normal contact force model and a Coulomb-type friction force model were utilized. The kinetic coefficient of friction was chosen as constant throughout the study. An innovative design-of-experiment (DOE)-based method for optimizing the performance of a mechanical system with the revolute joint clearance for different ranges of design parameters is then proposed. Based on the simulation model results from sample points, which are selected by a Latin hypercube sampling (LHS) method, a polynomial function Kriging meta-model is established instead of the actual simulation model. The reason for the development and use of the meta-model is to bypass computationally intensive simulations of a computer model for different design parameter values in place of a more efficient and cost-effective mathematical model. Finally, numerical results obtained from two application examples with different design parameters, including the joint clearance size, crank speed, and contact stiffness, are presented for the further analysis of the dynamics of the revolute clearance joint in a mechanical system. This allows for predicting the influence of design parameter changes, in order to minimize contact forces, accelerations, and power requirements due to the existence of joint clearance. [DOI: 10.1115/1.4026233]

Keywords: Revolute joint clearance, contact forces, multibody dynamics, Kriging meta-model, genetic algorithms

1 Introduction

In the past decade, many researchers have examined the optimal dynamical solution of different mechanical systems and mechanisms [1–3]. Additionally, different optimization methods have been implemented to obtain optimal solutions. In the study by Laribi et al. [2], a solution for the path generation problem in mechanisms was presented using the generic algorithm-fuzzy logic method. Selcuk et al. [3] proposed a neural-genetic method to investigate the effects of joints with clearance on its path generation and kinematic transmission quality. In order to reduce the computational complexity, the neural network has been used as a surrogate model in this study. The Genetic algorithm, as a global optimization method, has been widely used in many research fields, but its associated computational cost dramatically increases, especially for expensive model functions.

As a result of manufacturing tolerances, material deformations, and wear after a certain working period, clearances between mechanical components of mechanical systems occur in most kinematic joints. Excessive clearance values result in large contact forces at the joints, especially during high-speed mechanical operations. The presence of clearances leads to a decrease in the system reliability and durability of the system's components and machines [4,5]. Over the past decades, advances, mainly due to the development of intercross applications between computer-aided analysis of mechanical systems and optimization methodologies, have been achieved. These results could be utilized for the application of different mathematical programming techniques to the parametrical and topological syntheses and analyses of mechanical systems [6]. The optimization of mechanical system modeling with clearances can be used to bypass the computationally intensive simulation of the computer dynamic model. It also helps in the analysis, design, and control of the dynamic performance of a complex mechanical system and in quantifying the influence of clearance parameters.

During the past two decades, many studies on the influence of the joint clearance in planar and spatial multibody mechanical systems have been conducted. Dubowsky and Freudenstein developed the impact ring model, which is a simple model to demonstrate the effects of joint clearance in planar mechanisms [7]. Springs and dashpots were arranged in their model to predict the dynamics response of the mechanical system. Dubowsky and Moening quantified the interaction between the clearance joints and the mechanical system elasticity using a Scotch–Yoke simulation model [8]. Large impact forces developed at the clearance joints caused a failure in the Scotch–Yoke model. Furubashi and Morita presented a four-bar mechanism with multiple clearance revolute joints [9]. They analyzed and compared the results for

Contributed by the Design Engineering Division of ASME for publication in the JOURNAL OF COMPUTATIONAL AND NONLINEAR DYNAMICS. Manuscript received August 1, 2013; final manuscript received December 10, 2013; published online February 13, 2014. Assoc. Editor: Ahmet S. Yigit.

different numbers and various combinations of clearance joints and demonstrated the effect of clearances on the performance of the four-bar mechanism system.

Lankarani and Nikravesh extended the Hertz contact law to include a hysteresis damping function and represent the dissipated energy during impact [10]. A nonlinear continuous force acted on the model and the local indentation and relative penetration velocity was related to the contact force. Flores and his coworkers developed a precise model for the dynamic analysis of a mechanical system with dry and lubricated revolute joints [11–13]. The influences of the selected parameters on the dynamic response of mechanical systems with multiple clearance joints, including the clearance size, input crank speed, and number of joints modeled as clearance joints, were quantified in this study.

Mahrus designed a set of experimental investigations to show the performance of the journal bearing and the effect of the load diagram on hydrodynamic lubrication [14]. Different loads were applied to the test journal-bearing joint and both steady and varying unidirectional and full two-component dynamic loading were considered in the study. Wilson and Fawcett modeled a slider-crank mechanism with a clearance in the sliding bearing to measure the transverse motion of the slider [15]. They tested a number of parameters such as the geometry, speed, and mass distribution of the mechanical system, which influence the transverse motion and they derived the equation of motion with these parameters based on the results. Haines derived the equations of motion for a multibody mechanical system that describes the contributions at a revolute clearance joint with no lubrication present [16]. The study also included an experimental investigation on the dynamic response of revolute clearance joints. Under static loading, the deflection associated with contact elasticity in the dry journal-bearing joint was found to be much greater and linear than predicted [17]. Bengisu et al. developed a four-bar mechanism based on zero-clearance analysis to compare the theoretical results with the experimental results [18]. A model with multiple joints was used in clearances to study contact energy loss in the mechanical system.

Feng et al. developed a method for optimizing the mass distribution of planar linkage with clearance joints to control the change of inertia forces [19]. Tsai and Lai investigated the kinematic sensitivity of the transmission performance of linkages with joint clearances [20]. In their study, loop-closure equations were used in the position analysis of a four-bar mechanism in which all joints have clearances. Yildirim et al. predicted the transmission angle of a slider-crank mechanism with an eccentric connector based on neural networks [21]. The neural network structure was a feed-forward network and the best approximation was obtained with five types of algorithms. Erkaya and Uzmay studied the effects of joint clearances on the performance of a mechanism in terms of path generation and transmission angle, using neural networks and genetic algorithms (GAs), respectively [3,21].

A computer-aided analysis of multibody mechanical systems is utilized in this study as a simulation model. The goal of this study is to use the Kriging mathematical model as a design-of-experiments optimization tool, in order to demonstrate the influence of the design variables on the dynamic performance of mechanical systems with revolute clearance joints. The reason the Kriging model was used in this research is that the computer simulation for a given set of design parameters is usually quite computationally intensive and each simulation for a given set of design variables could take extensive computation time. Because there are wide ranges of values in the design variables such as the clearance sizes, ratios of length, material properties, contact stiffnesses, and speeds of operation, studying the effects of each of these variables would take enormous computational time and effort.

In the present study, the mathematical formulation of the revolute clearance joint is fully described and the relationship between the design parameters and contact forces in joints is examined. First, the classical slider-crank mechanical system is modeled and simulated in MSC.ADAMS and the performance of the system with different sets of parameters is examined. Next, the theoretical basis of the methods are stated, illustrating the framework for the DOE methods of the Latin hypercube sampling, Kriging metamodel, and genetic algorithm. Next, two simple examples are presented using these previous methods to further expand the analysis of the dynamic behavior of the mechanism with the revolute clearance joint at different ranges of the design parameters.

2 Modeling Revolute Joints With Clearance

A revolute joint with clearance, as shown in Fig. 1, can be described as a movable journal assembled inside a bearing, with the journal's and bearing's radii of R_J and R_B, respectively. In reality, there is a clearance between the journal and the bearing in mechanical systems in order to cause a relative motion between the two. The journal can move inside the bearing and this will add some degrees of freedom to the system. The difference between the radius of the bearing and the radius of the journal is the radial clearance size c. The penetration between the bearing and journal appears when they are in contact.

The indentation depth due to the contact impact between the journal and the bearing can be defined as

$$\delta = e - c \tag{1}$$

where e is the magnitude of the eccentricity and c is the radial clearance. The eccentricity is evaluated as

$$e = \sqrt{\Delta X^2 + \Delta Y^2} \tag{2}$$

where ΔX and ΔY are the horizontal and vertical displacements, respectively, measured from the state when the centers of the

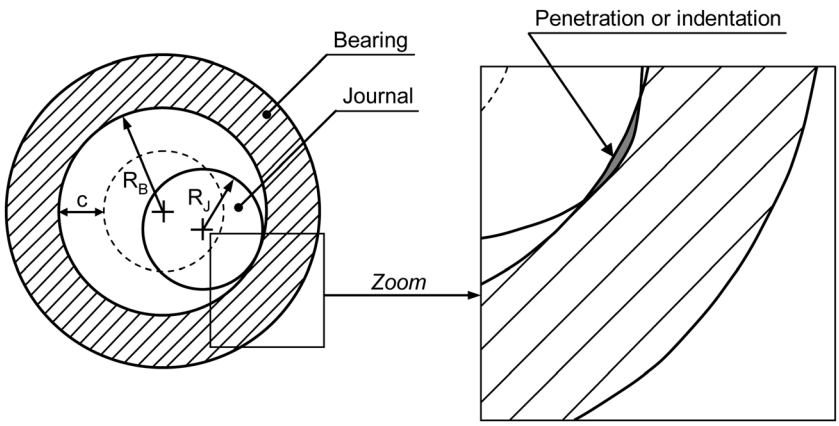

Fig. 1 Revolute joint with clearance (clearance exaggerated for clarity)

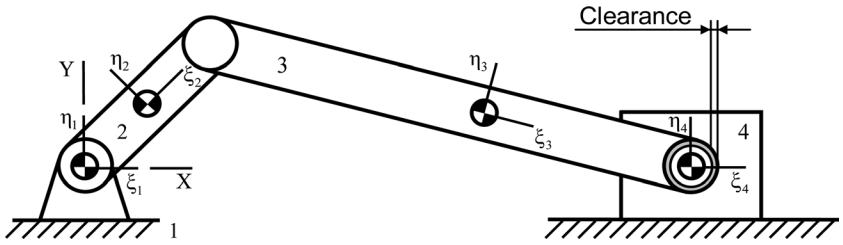

Fig. 2 Slider-crank mechanism with clearance joint

Table 1 Geometric and inertial properties of mechanism

Body number	Length (m)	Mass (kg)	Moment of inertia (kg m^2)
2	0.05	0.30	0.00010
3	0.12	0.21	0.00025
4	0.06	0.14	0.00010

journal and the bearing coincide. In turn, the radial clearance is defined as

$$c = R_B - R_J \tag{3}$$

Two situations can occur at the joint. In the first case, when the journal does not make contact with the bearing and the penetration depth is a negative value, the journal has a free-flight motion inside the bearing and, thus, there is no contact-impact force developed at the joint. In the second case, when the journal contacts with the bearing wall, a contact force between the journal and the bearing is developed in the direction of the centers of the bearing and the journal [4] and the indentation depth value will be greater than zero.

The contact-impact force F_N, in relation to the penetration indentation, can be modeled by the Hertz law as [10]

$$F_N = K\delta^n \tag{4}$$

where K is the stiffness coefficient and δ is the indentation depth given by Eq. (1). The exponent n is usually set for analysis in the range of 1.5–2.5 for most metal-to-metal contact. The stiffness coefficient K depends on the material properties and the contacting surface and is defined as

$$K = \frac{4}{3(\sigma_B + \sigma_J)}\left[\frac{R_B R_J}{R_B - R_J}\right]^{1/2} \tag{5}$$

The material parameters σ_B and σ_J are defined as

$$\sigma_k = \frac{1-\nu_k^2}{E_k} \quad (k = B, J) \tag{6}$$

where the variables ν_k and E_k are Poisson's ratio and Young's modulus, respectively, for the journal and the bearing.

The Hertz law given by Eq. (4) does not include any energy dissipation. Lankarani and Nikravesh [10] extended the Hertz model to include a hysteresis damping function as follows:

$$F_N = K\delta^n\left[1 + \frac{3(1-c_e^2)}{4}\frac{\dot{\delta}}{\dot{\delta}^{(-)}}\right] \tag{7}$$

where the stiffness coefficient K can be obtained from Eqs. (5) and (6)], c_e is the restitution coefficient, $\dot{\delta}$ is the relative penetration velocity, and $\dot{\delta}^{(-)}$ is the initial impact velocity.

3 A Multibody System With Joint Clearance

In this section, a computer model for the classic slider-crank mechanism with one revolute clearance joint is considered in order to analyze the dynamic behavior of the mechanical system. Figure 2 shows the configuration of the slider-crank mechanism, which comprises four bodies that represent the crank, connecting rod, slider, and ground. In this case, the multibody model has only one clearance joint. There are four joints: two ideal revolute joints between the ground and the crank and the crank and the connecting rod; one ideal translational joint between the slider and ground; and one nonideal revolute joint clearance between the connecting rod and slider. The geometric and inertia properties of each body in this system are shown in Table 1 [17]. The moment of inertia is taken with respect to the center of gravity of the body.

A model of the slider-crank mechanism is constructed in MSC.ADAMS, as shown in Fig. 3. In the model, all bodies are considered to be rigid. The initial crank angle and velocity of the journal

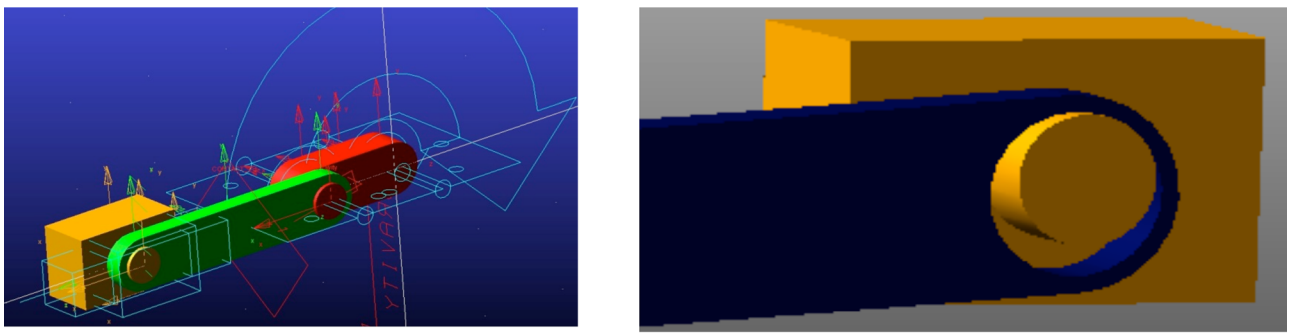

(a) (b)

Fig. 3 (*a*) Model of the slider-crank mechanism developed in MSC. ADAMS, and (*b*) exaggerated joint clearance at the piston pin

Table 2 Parameters used in dynamic simulation of slider-crank mechanism with clearance joint

Nominal-bearing radius	10.0 mm
Journal-bearing width	40.0 mm
Restitution coefficient	0.9
Friction coefficient	0.0
Young's modulus	207 GPa
Poisson's ratio	0.3
Baumgarte α, β	5
Total simulation time	0.24 s
Total steps	50,000

center are set to zero and the journal and bearing centers are coincident. The dynamic parameters used in the simulation are listed in Table 2.

Comparing the results from this MSC.ADAMS computer simulation model (Fig. 4) with the experimental results of the slider-crank mechanism obtained by Flores et al. [22] (see Fig. 5) indicates a similar pattern between the computer model in this study and the experimental results. Hence, the slider-crank mechanism model from this study can simulate the dynamic behavior of the system with reasonable accuracy. This simulation model will be utilized here. The values for the radial clearance size and the input crank speed are used for investigating the impact of the revolution clearance joint in the slider-crank mechanical system.

As shown in Figs. 6–8, the results of the slider acceleration, contact force at the clearance, and crank reaction force demonstrate different dynamic behaviors of the slider-crank mechanism with different values of the radial clearance; namely, 0.05 mm, 0.1 mm, 0.2 mm, and 0.5 mm. The crank rotates with a 2000 rpm constant angular speed. The results indicate that when the clearance size is increased, the curves become noisier and the dynamic behavior tends to be nonperiodic. As the clearance size decreases, the dynamic behavior tends to be closer to ideal. Those plots typically reach the highest value when the crank angle is at multiples of 180 deg rotation, which is when the slider is in the critical position. These observations can also be confirmed in the plots of the joint reaction forces shown in Figs. 7 and 8. As can be seen, when the clearance size is increased, the contact force and required crank input power are significantly increased.

Figures 9–11 show the influence of the crank angular speed. The values chosen for the crank speed are 200 rpm, 1000 rpm, 2000 rpm, and 5000 rpm. In this set, the clearance size is set to 0.1 mm. The different behaviors of the slider acceleration and the joint reaction force are displayed in these plots. The decrease in crank speed results in the curves having more noise and higher peak values for the slider acceleration.

4 Kriging Model-Based Optimization

This section presents a procedure for constructing an objective function using the Kriging model. In the first part, the Latin

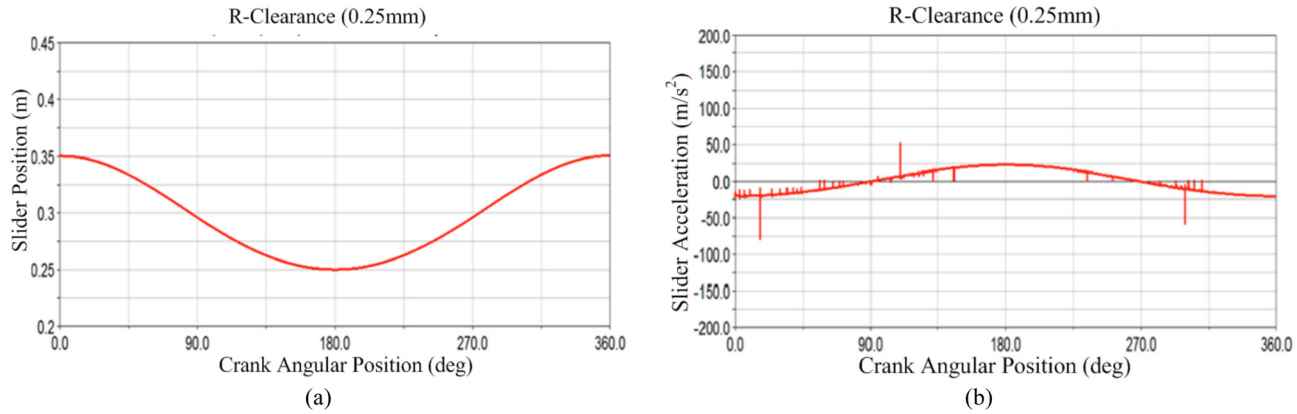

Fig. 4 Dynamic response of the slider-crank from MCS.ADAMS modeling with a crank speed of 200 rpm: (*a*) slider position for a clearance of 0.25 mm, and (*b*) slider acceleration for a clearance of 0.25 mm

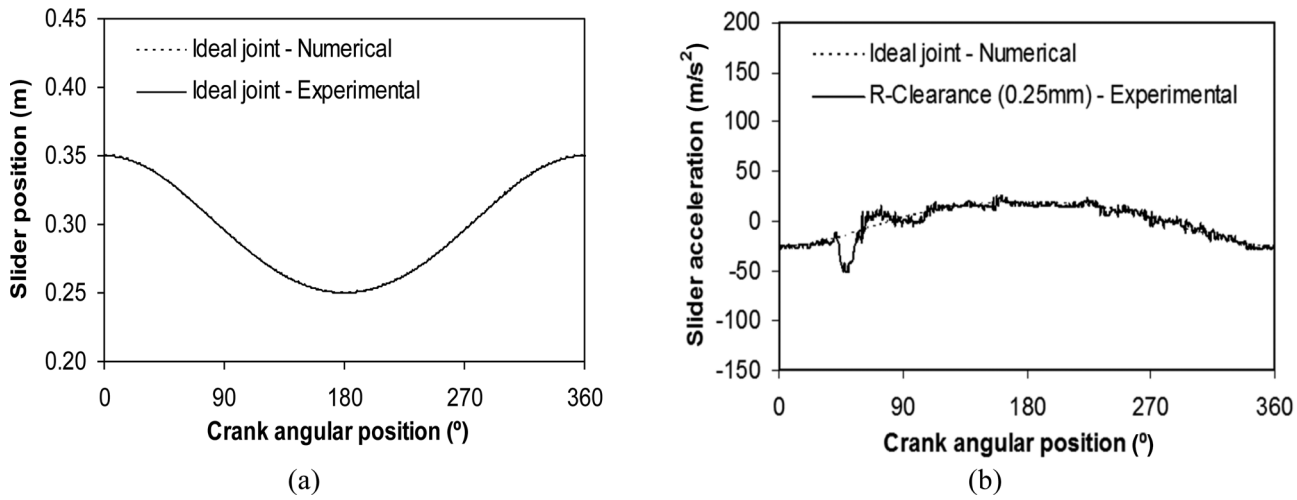

Fig. 5 Dynamic response of the experimental slider-crank from Ref. [22] with a crank speed of 200 rpm: (*a*) slider position for a clearance of 0.25 mm, and (*b*) slider acceleration for a clearance of 0.25 mm

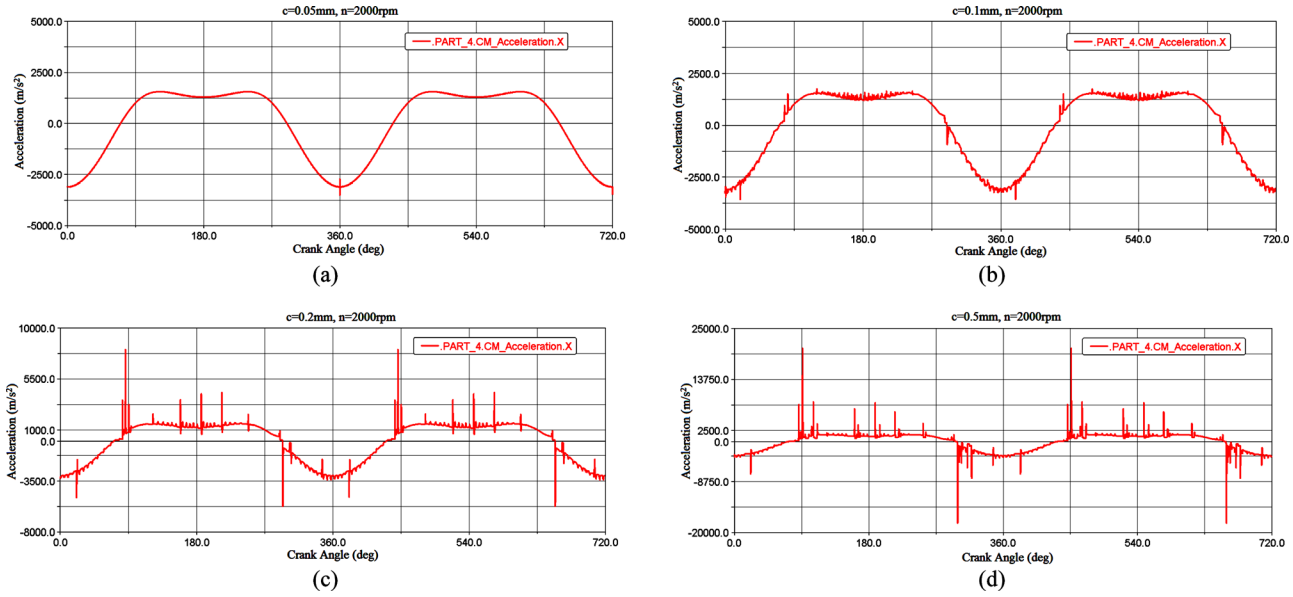

Fig. 6 Slider acceleration for different clearance sizes: (*a*) 0.05 mm, (*b*) 0.1 mm, (*c*) 0.2 mm, and (*d*) 0.5 mm

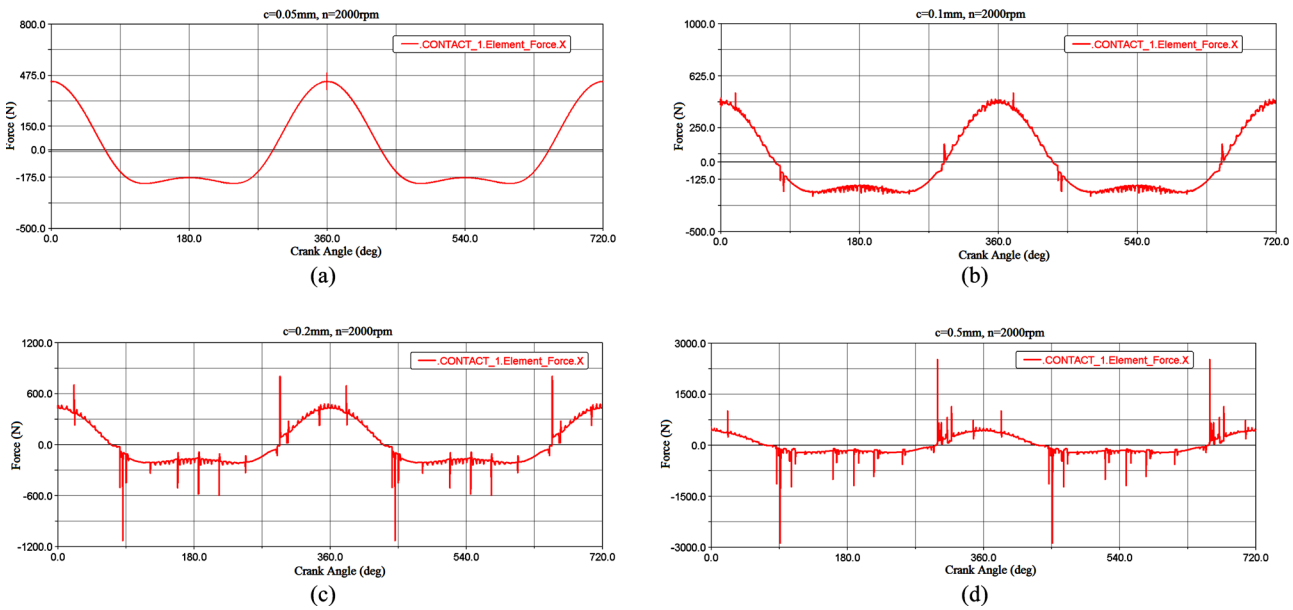

Fig. 7 Contact force for different clearance sizes: (*a*) 0.05 mm, (*b*) 0.1 mm, (*c*) 0.2 mm, and (*d*) 0.5 mm

hypercube is introduced for acquiring the initial design points. After locating several initial design points, their performance data can be obtained by the computer simulation experiment (MSC.ADAMS). Each computer simulation for a given set of deign parameters requires up to 50,000 numerical integration steps for one complete crank rotation, which is quite inefficient and computationally intensive; therefore, the Kriging model is developed and utilized instead in this research to optimize the process. The objective here is to develop a prediction model to estimate the value of the objective function for any given design point in the design space using the Kriging model instead of the computer simulation experiment. For this purpose, the Kriging model can be constructed based on the initial design points and their performances. The implementation of the method is shown in Fig. 12. The Kriging model is constructed by using the results from sample points coming from individual computer simulations. A genetic algorithm is used to obtain optimal results on the design parameter.

The neural network and Kriging model are two potential techniques, among others, and both can capture the unknown nonlinearity in the system performance. Based on a study by Yuan and Bai [1], in which they compared the neural network and Kriging model, the Kriging model can usually produce meta-model optima that are superior in precision. Additionally, for a given sample size, the Kriging model tends to provide a better overall fit than the neural networks.

In this research, the objective is to utilize a nonparameter Kriging model to predict the dynamic response for any given design point within the design space. In order to construct the surrogate Kriging model, several points inside the design space must first be utilized and their corresponding responses must be obtained at these points first, using the computer simulations (here, ADAMS). The constructed Kriging model can then be used as a surrogate model instead of the computer simulation model, in order to predict the response at any other design point within the design space. In addition to the use of the Kriging model for the prediction of

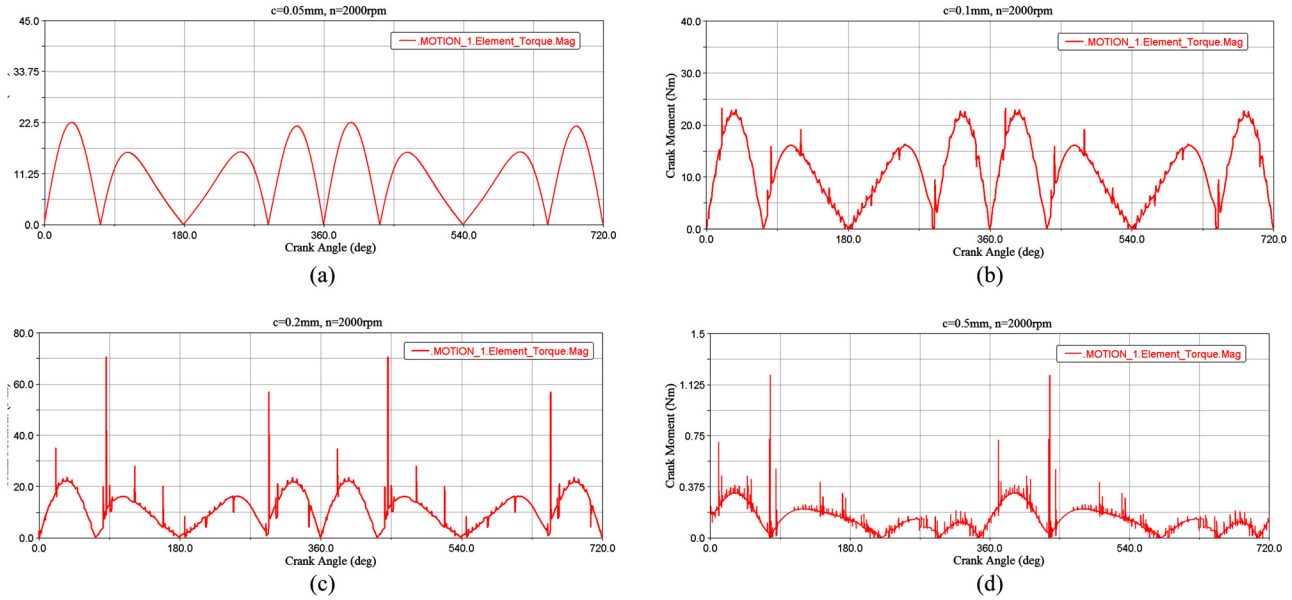

Fig. 8 Crank moment for different clearance sizes: (*a*) 0.05 mm, (*b*) 0.1 mm, (*c*) 0.2 mm, and (*d*) 0.5 mm

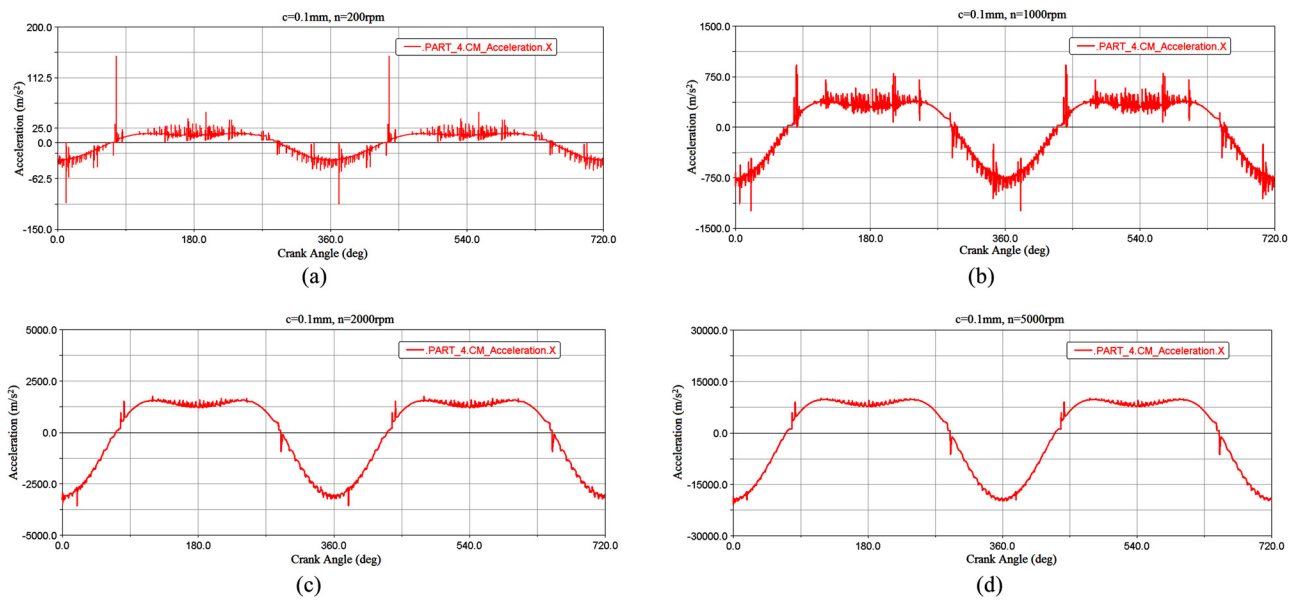

Fig. 9 Slider acceleration for different crank speeds: (*a*) 200 rpm, (*b*) 1000 rpm, (*c*) 2000 rpm, and (*d*) 5000 rpm

the response at different design points, the scheme allows the visualization of the trends of the response surfaces when the design variables are changed.

4.1 Latin Hypercube Sampling. In order to acquire a set of initial samples from the ranges of the parameter variables to confine the number of simulations, the LHS is used to ensure that each value of a variable is equally important in the sample. This method not only reduces the number of simulations but also retains the proper orthogonality and proportionality of the sample. The Latin hypercube is a statistical method for placing M sample points, which are divided into equally probable intervals in every variable, when a function has N variables. In addition, the M sample points must be satisfied by the Latin hypercube requirement that each sample is the only one in each axis-aligned hyper-plane containing it [23].

4.2 Kriging Model. The Kriging model is a nonparametric interpolation model for integrating the given sample points to approximate the model parameters and forecasting the unknown response of a new design point [24–26]. Considering a performance function with k random inputs, a Kriging model can be constructed with n samples, which is (x_i, y_i), where $x_i = (x_i^1 \ldots x_i^n)$, $i = 1,\ldots,n$ are simple inputs and y_i is the system performance when the system is given the inputs x_i. The term x_i^n represents the nth design point for input x_i.

In the Kriging model, system performances are generated from the following:

$$Y(x) = f(x) + G(x) \tag{8}$$

where $Y(x)$ is the unknown function, $f(x)$ is a polynomial function of x, and $G(x)$ is the realization of a Gaussian stochastic process with zero mean and variance σ^2. The polynomial term $f(x)$ is simplified by a constant value μ. Hence, the Kriging model can be rewritten as

$$Y(x) = \mu + G(x) \tag{9}$$

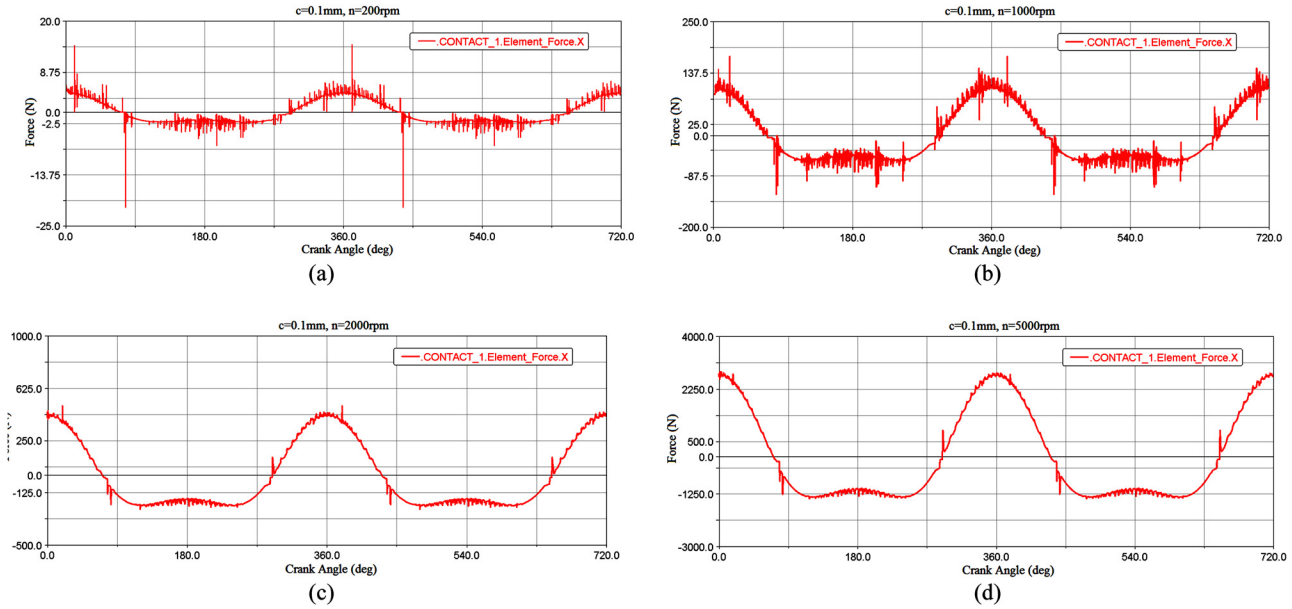

Fig. 10 Contact force for different crank speeds: (*a*) 200 rpm, (*b*) 1000 rpm, (*c*) 2000 rpm, and (*d*) 5000 rpm

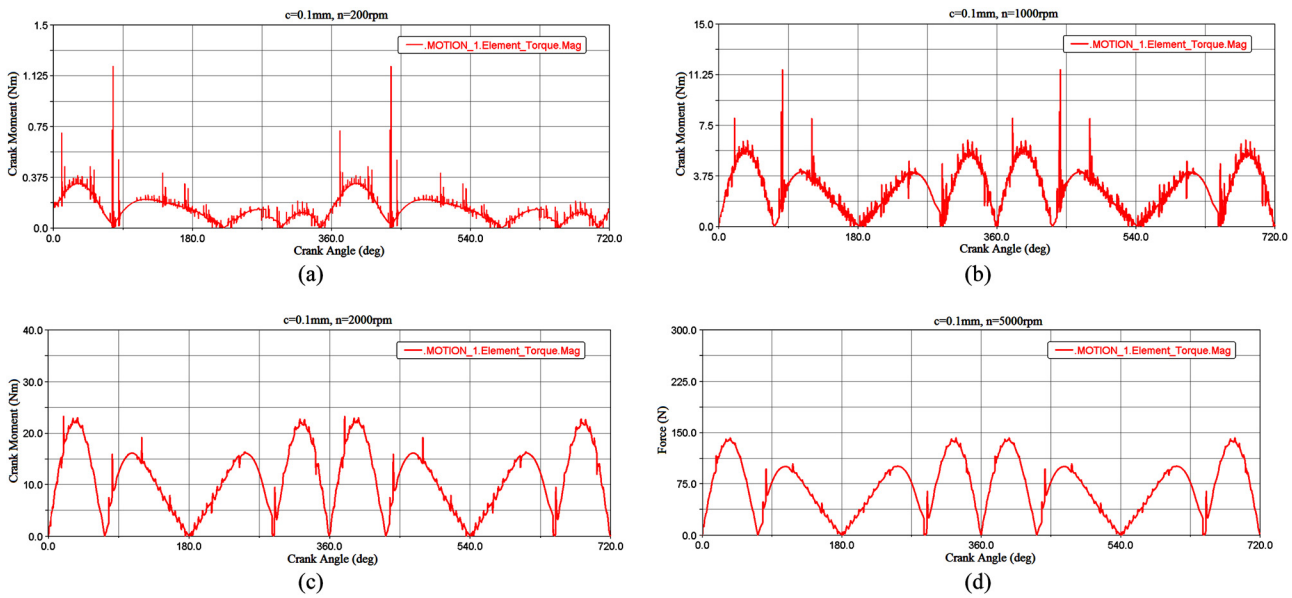

Fig. 11 Crank moment for different crank speeds: (*a*) 200 rpm, (*b*) 1000 rpm, (*c*) 2000 rpm, and (*d*) 5000 rpm

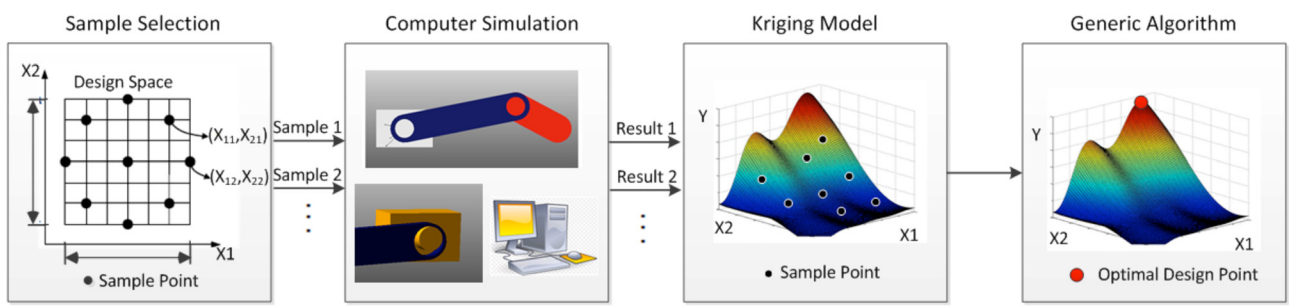

Fig. 12 Flow chart for implementation of the DOE and Kriging-based optimization model

The entry correlation matrix for $G(x)$ is given by [16]

$$\mathrm{Corr}\left[G\left(x_i, x_j\right)\right] = \sigma^2 R\left(x_i, x_j\right) \tag{10}$$

where $R(x_i, x_j)$ represents the (i, j) entry of an $n \times n$ matrix and this correlation matrix is defined by the distance between two sample points x_i, x_j with ones along the diagonal, which can be expressed as

$$R\left(x_i, x_j\right) = \exp\left[-\sum_{p=1}^{k} \theta_p \left|x_i^p - x_j^p\right|^{\alpha_p}\right] \tag{11}$$

The term inside the exponential is the distance between the two designed sample points (x_i, x_j), and θ_p and α_p are two parameters that must be determined in order to make a proper prediction using the Kriging model. With n sample points (x_i, x_j), the likelihood function of the model parameters can be given as

$$\text{Likelihood} = -\frac{1}{2}\left[n\ln(2\pi) + n\ln\sigma^2 + \ln|R| + \frac{1}{2\sigma^2}(y - A\mu)^T R^{-1}(y - A\mu)\right] \tag{12}$$

where y is the column vector of the response and A is a $n \times 1$ vector filled with ones. The term μ can be estimated as

$$\mu = [A^T R^{-1} A]^{-1} A^T R^{-1} y \tag{13}$$

The σ^2 also can be estimated as [21]

$$\sigma^2 = \frac{(y - A\mu)^T R^{-1}(y - A\mu)}{n} \tag{14}$$

With the preceding two equations, the likelihood function is transformed into a function, which depends only upon the parameters θ_p and α_p. In addition, these two parameters can be determined by maximizing the likelihood function and, therefore, the correlation matrix R can be calculated. With this prediction model, the system performance can be estimated for any given design point x^* as

$$Y(x^*) = \mu + r^T(x^*) R^{-1}(y - A\mu) \tag{15}$$

where $r(x^*)$ is the correlation vector between the prediction point x^* and the design points
x_1–x_n, which is given by

$$r^T(x^*) = [\mathrm{Corr}[G(x^*, x_1)], \ldots, \mathrm{Corr}[G(x^*, x_n)]] \tag{16}$$

4.3 Example Use of Kriging Model. In order to explain the sampling method and the Kriging model, a mathematical model, which is shown as the Branin function, is considered in term of two variables x_1 and x_2 as [27]

$$Y(x) = \left(x_2 - \frac{5.1}{4\pi^2}x_1^2 + \frac{5}{\pi}x_1 - 6\right)^2 + 10\left[\left(1 - \frac{1}{8\pi}\right)\cos x_1 + 1\right]$$
$$x_1 \in [-5, 10]$$
$$x_2 \in [0, 15] \tag{17}$$

In the first step of this example, 20 design points are selected by LHS, as shown in Fig. 13.

Figure 14(*a*) shows what the entire model looks like as a meta-model and the 20 design points are shown in the image as small dots. In Fig. 14(*b*), a surrogate model is built using the Kriging model. The Kriging model with these 20 design points has been used to assume the response surface. Comparing this to the exact results, the Kriging model uses only 20 design points to obtain acceptable and reasonably accurate results.

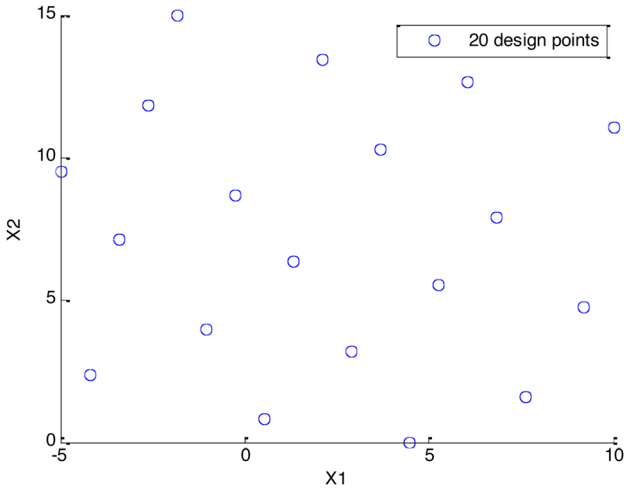

Fig. 13 Design points selected by the LHS

Among the interpolation methods, the neural network and Kriging model are two potential techniques, among others, and both can capture the unknown nonlinearity in the system performance. Based on a study by Yuan and Bai [1], in which they compared the neural network and the Kriging model, the Kriging model can usually produce meta-model optima that are superior in precision. Additionally, for a given sample size, the Kriging model tends to provide a better overall fit than the neural networks.

4.4 Genetic Algorithm. Genetic algorithms are nongradient-based methods [28] that can generate a global promising result for a complex optimization problem. In most cases, the GA is divided into three steps: evaluation, crossover, and mutation. An initial population of the design variable is selected by some cost functions. Then the initial population is changed depending on the fitness function and, using a crossover strategy and mutation, a new generation of population is created. This process continues until the fitness function converges to the global optimal point. The input variables for this point will be the strongest population selected by the evolution. Compared to the gradient method, a GA can successfully avoid local minima since it tests the design points over a large domain in global space. However, this method is computationally expensive, especially when it is applied to computer simulation models. In order to overcome this weak point and to compensate for the expensive optimization process, this research replaces the ordinary computer simulation model with the cost-effective Kriging model. The objective functions considered in this study are as follows:

$$\min\{\ddot{x}_{\text{slider}}\}_{\max} \tag{18}$$

$$\min\{F_N\}_{\max} \tag{19}$$

$$\min\{P\}_{\max} \tag{20}$$

where $\ddot{x}_{\text{slider}}$, F_N, and P are, respectively, the acceleration of the slider block, the contact force at the pin, and the power input requirement for the operation of the mechanism. The power is calculated as the product of the input torque T and crank angular velocity ω, i.e.

$$P = T\omega \tag{21}$$

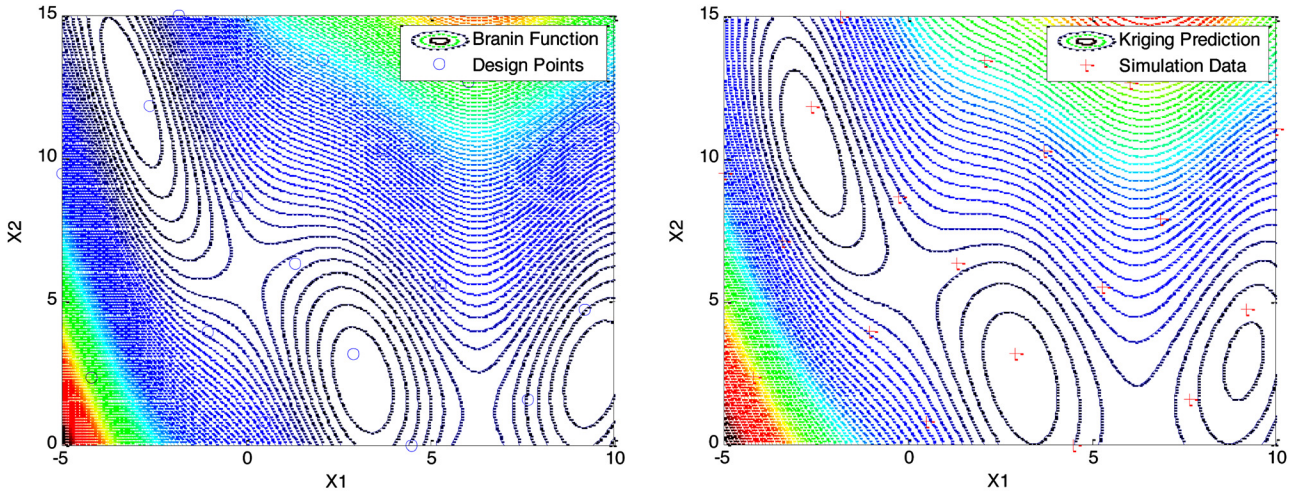

Fig. 14 (*a*) Exact model of the Branin function, and (*b*) surrogate model predicted by the Kriging model

5 DOE- and Kriging-Based Study of Slider-Crank Mechanism

In this section, the dynamic behavior of the slider-crank mechanical system with a revolute clearance joint will be studied further, using two simple examples that use the DOE method introduced in the previous sections. The Kriging meta-model is constructed in order to optimize and analyze the computer simulation experiment process and the genetic algorithm is used to find the minimal contact force in the joint by controlling appropriate values of the design parameters. The implementation of this method was previously shown in Fig. 12. Sample points are selected from design variables by the LHS and the slider-crank mechanism model developed in the previous section is used to evaluate performances acquired from the sample points. Then the absolute maximum value for dynamic behavior such as the contact forces, slider accelerations, crank moment, and power consumption, all from the simulation model, can be treated as the system performance and a surrogate model is built using the Kriging meta-model to replace the expensive computer simulation model. The remaining quantitative values from the objective functions can be predicted by the Kriging model. The GA is then used to optimize the results. In the process, the dynamic behavior of the mechanical system with a revolute clearance joint case is obtained for a range of design parameters.

5.1 Demonstrative Example 1. An illustrative example is presented here to investigate the influence of the radial clearance size and the material/contact stiffness coefficient on the dynamic behavior of the slider-crank mechanism with a revolute clearance joint. The computer simulation model built in MSC.ADAMS is used in this experiment. A constant input speed of 5000 rpm is set up on the crank. At a high constant input speed, contact forces at the joint can also become quite large and the impact of the change of the clearance size and stiffness coefficient can be more visible on the dynamic response of the system. Since the system is dynamically quite stiff due to the existence of large contact forces, which act and disappear for a very short period of time, the numerical integrator used in the study is the enhanced GSTIFF integrator, developed Gear [29]. A variable integration time step selection scheme was chosen for the simulations with a reporting time step of 10^{-6} s [30].

Table 3 shows the radial clearance size and material/contact coefficient, which are selected as the design variables, and that the slider acceleration, contact force in the revolution joint, and the power consumption are investigated as the objective functions. The diametric clearance size of the nonideal revolute joint drops in the interval between 0.05 mm and 0.5 mm, which corresponds to the clearance size in a typical journal-bearing. For the stiffness coefficient, common steel and iron alloys are chosen as experimental materials. Young's modulus of metal is taken to be between 113 GPa and 210 GPa and Poisson's ratio falls into the region between 0.23 and 0.3. The stiffness coefficient is taken to be between $3.4 \times 10^{+9}$ N/m$^{1.5}$ and $1.7 \times 10^{+9}$ N/m$^{1.5}$.

Ten design points were generated by the Latin hypercube method (see Table 4) and inserted in the simulation model to evaluate the objective functions. In Fig. 15, the surface plots are acquired by utilizing the Kriging model.

After the Kriging model is built by following the methodology, in order to detect its accuracy, another point (the 11th point) is used as the clearance size of 0.18 mm and the contact stiffness of $1.0 \times 10^{+10}$ N/m$^{1.5}$. Both the computer simulation model and Kriging meta-model are used to examine the highest absolute value of the slider acceleration of the slider-crank mechanism. The result for the highest absolute value of slider acceleration

Table 3 General experiment objects in example 1

Design variables	1. Radial clearance size (mm)	0.05–0.5
	2. Material/contact stiffness coefficient (N/m$^{1.5}$)	$3.4 \times 10^{+9}$–$1.7 \times 10^{+9}$
Objective functions	1. Slider acceleration	
	2. Contact force at joint clearance	
	3. Power consumption	

Table 4 Sample points and the computer simulation results

Sample number	Clearance size (mm)	Stiffness (N/m$^{1.5}$)	Slider acceleration (m/s^2)	Contact force (N)	Power (W)
1	0.5	$9.4 \times 10^{+9}$	$1.1 \times 10^{+5}$	$1.5 \times 10^{+4}$	$1.2 \times 10^{+5}$
2	0.45	$3.4 \times 10^{+9}$	$1.0 \times 10^{+5}$	$1.4 \times 10^{+4}$	$0.9 \times 10^{+5}$
3	0.05	$1.5 \times 10^{+10}$	$2.0 \times 10^{+4}$	$2.7 \times 10^{+3}$	$1.9 \times 10^{+4}$
4	0.3	$1.1 \times 10^{+10}$	$8.5 \times 10^{+4}$	$1.2 \times 10^{+4}$	$8.2 \times 10^{+4}$
5	0.15	$1.2 \times 10^{+10}$	$2.7 \times 10^{+4}$	$3.7 \times 10^{+3}$	$2.5 \times 10^{+4}$
6	0.35	$6.4 \times 10^{+9}$	$9.3 \times 10^{+4}$	$1.3 \times 10^{+4}$	$9.1 \times 10^{+4}$
7	0.25	$1.7 \times 10^{+10}$	$6.8 \times 10^{+4}$	$9.6 \times 10^{+3}$	$6.2 \times 10^{+4}$
8	0.1	$7.9 \times 10^{+9}$	$2.0 \times 10^{+4}$	$2.8 \times 10^{+3}$	$1.8 \times 10^{+4}$
9	0.2	$4.9 \times 10^{+9}$	$4.5 \times 10^{+4}$	$6.3 \times 10^{+3}$	$4.3 \times 10^{+4}$
10	0.4	$1.4 \times 10^{+10}$	$9.1 \times 10^{+4}$	$1.3 \times 10^{+4}$	$9.3 \times 10^{+4}$

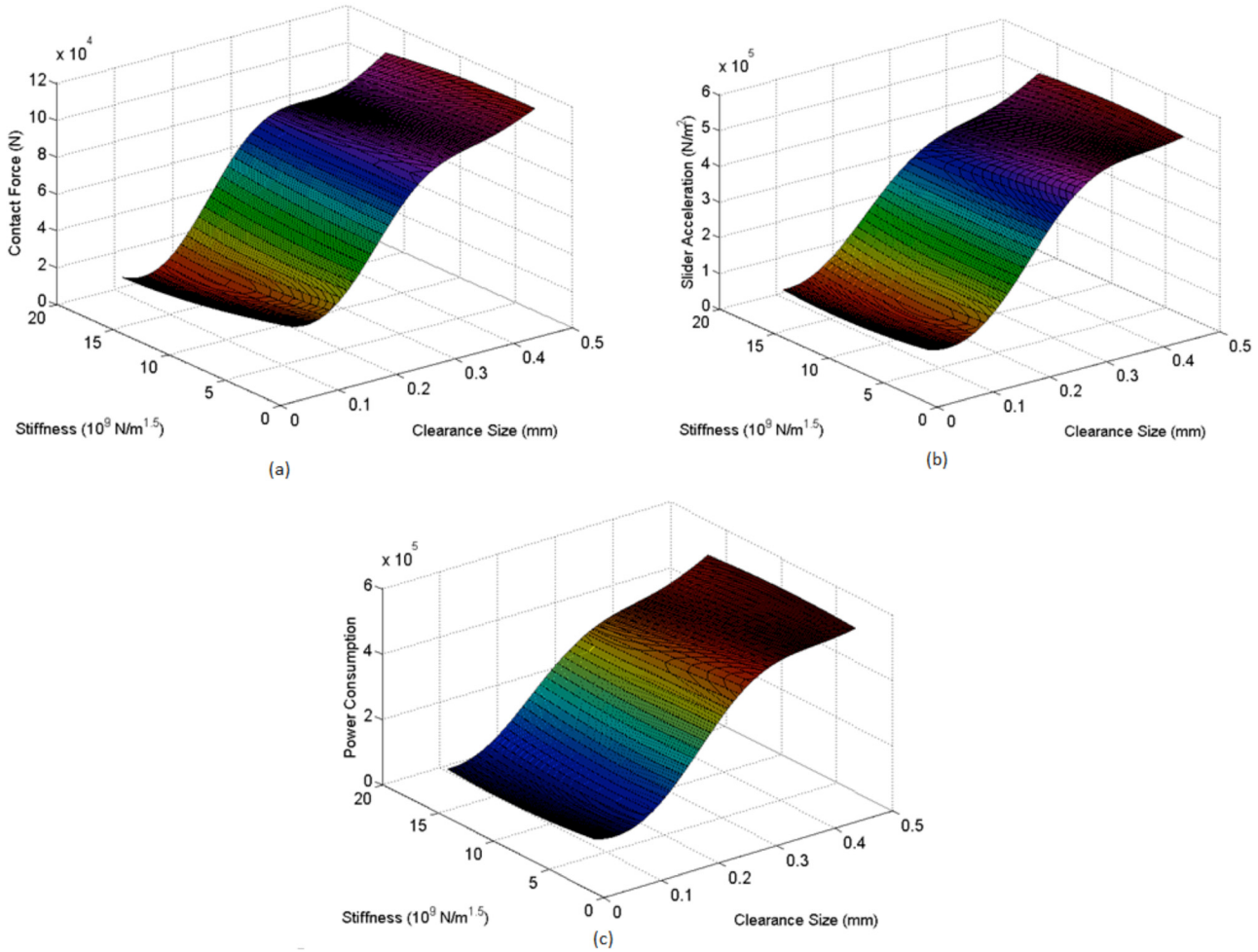

Fig. 15 (*a*) Surface plot for joint contact force, (*b*) surface plot for slider acceleration, and (*c*) surface plot for crank power consumption

from the computer simulation model is $3.2 \times 10^{+4}$ m/s^2. The highest absolute value of slider acceleration from the Kriging model is $3.0 \times 10^{+4}$ m/s^2. The results indicate that the respective error for the highest absolute value of acceleration for the Kriging model is within 6% of the actual value. Hence, the Kriging model can reasonably predict the response of this system for the studied range of parameters.

Figure 15(*a*) presents the contact force between the bearing and journal for the dynamic response histories as the functions of the clearance size and the stiffness coefficient. Figures 15(*b*) and 15(*c*) show the surface plots for the slider acceleration and power consumption. From Fig. 15, it is clear that the contact force grows monotonically as the clearance size increases at the center of the image and the change gradually becomes smooth when the curve tends to the edge of the image. In addition, the clearance size is more sensitive than the stiffness in the studied range. The results for the slider acceleration show similar phenomena on the contact force. After applying the genetic algorithm, the optimal point is found to have a material stiffness coefficient of $3.4 \times 10^{+4}$ N/m$^{1.5}$ and a radial clearance size of 0.05 mm. The results from this DOE-based study show that the lowest values in the range of design variables are optimal. In the next demonstrative example, a larger range of design variables will be selected to investigate the dynamic response of the same system.

5.2 Demonstrative Example 2. In this section, another example of the use of the DOE and Kriging model is presented in order to illustrate the dynamic response of the revolute clearance joint. The same slider-crank mechanical system is also used in this experiment, but three input design variables are utilized instead. For this analysis, the three design variables are the input crank speed, material stiffness, and size of the radial joint clearance and the objective functions are the contact force between the bearing and the journal and the power consumption (see Table 5). The larger ranges of the parameter variables are given in the example, because the diametric clearance size is chosen in the interval between 0.02 mm and 1 mm, the range of the stiffness coefficient is taken between $3.3 \times 10^{+8}$ N/m$^{1.5}$ and $3.3 \times 10^{+11}$ N/m$^{1.5}$, and the value of the crank speed is chosen between 50 rpm and 5000 rpm.

The LHS is used to choose the 30 sample points. Importing the samples in the simulation model, the absolute maximum values for the objective functions are shown in Table 6.

The data from Table 6 are used to build the Kriging metamodel. The Kriging model is established as a prediction model to estimate the objective function for any given design point and it is

Table 5 General experiment objects in example 2

Design variables	1. Input crank speed (rpm)	50–5000
	2. Material/contact stiffness coefficient (N/m$^{1.5}$)	$3.3 \times 10^{+8}$–$3.3 \times 10^{+11}$
	3. Radial clearance size (mm)	0.02–1.00
Objective functions	1. Contact force at joint clearance	
	2. Power consumption	

Table 6 Sample points and the computer simulation results

Sample number	Crank speed (rpm)	Stiffness ($N/m^{1.5}$)	Clearance size (mm)	Contact force (N)	Acceleration (m/s^2)	Power (W)
1	$7.33 \times 10^{+2}$	$2.16 \times 10^{+11}$	0.76	$9.03 \times 10^{+2}$	$6.45 \times 10^{+3}$	$4.30 \times 10^{+3}$
2	$5.00 \times 10^{+1}$	$2.31 \times 10^{+10}$	0.39	$1.32 \times 10^{+1}$	$9.40 \times 10^{+1}$	$1.40 \times 10^{+4}$
3	$3.80 \times 10^{+3}$	$2.62 \times 10^{+11}$	0.63	$9.24 \times 10^{+3}$	$6.60 \times 10^{+4}$	$2.18 \times 10^{+5}$
4	$3.12 \times 10^{+3}$	$9.13 \times 10^{+10}$	0.8	$8.45 \times 10^{+3}$	$6.35 \times 10^{+4}$	$1.61 \times 10^{+5}$
5	$3.30 \times 10^{+3}$	$1.59 \times 10^{+11}$	0.05	$1.19 \times 10^{+3}$	$8.48 \times 10^{+3}$	$2.09 \times 10^{+4}$
6	$1.07 \times 10^{+3}$	$1.94 \times 10^{+11}$	0.19	$5.00 \times 10^{+2}$	$3.57 \times 10^{+3}$	$5.30 \times 10^{+3}$
7	$2.62 \times 10^{+3}$	$3.30 \times 10^{+8}$	0.49	$5.03 \times 10^{+3}$	$3.59 \times 10^{+4}$	$8.58 \times 10^{+4}$
8	$9.03 \times 10^{+2}$	$1.17 \times 10^{+10}$	0.7	$1.11 \times 10^{+3}$	$7.92 \times 10^{+3}$	$5.06 \times 10^{+3}$
9	$2.78 \times 10^{+3}$	$2.96 \times 10^{+11}$	0.09	$9.26 \times 10^{+2}$	$6.61 \times 10^{+3}$	$1.34 \times 10^{+4}$
10	$5.62 \times 10^{+2}$	$3.07 \times 10^{+11}$	0.56	$6.79 \times 10^{+2}$	$4.80 \times 10^{+3}$	$1.80 \times 10^{+3}$
11	$2.43 \times 10^{+3}$	$2.39 \times 10^{+11}$	0.53	$4.80 \times 10^{+3}$	$3.43 \times 10^{+4}$	$6.30 \times 10^{+4}$
12	$1.25 \times 10^{+3}$	$1.37 \times 10^{+11}$	0.97	$1.83 \times 10^{+3}$	$1.30 \times 10^{+3}$	$1.50 \times 10^{+4}$
13	$4.15 \times 10^{+3}$	$1.48 \times 10^{+11}$	0.59	$9.05 \times 10^{+3}$	$6.46 \times 10^{+4}$	$2.52 \times 10^{+5}$
14	$4.83 \times 10^{+3}$	$3.44 \times 10^{+10}$	0.12	$2.89 \times 10^{+3}$	$2.06 \times 10^{+4}$	$7.28 \times 10^{+4}$
15	$2.95 \times 10^{+3}$	$3.19 \times 10^{+11}$	0.9	$8.83 \times 10^{+3}$	$6.30 \times 10^{+4}$	$1.82 \times 10^{+5}$
16	$3.98 \times 10^{+3}$	$1.03 \times 10^{+11}$	0.22	$5.02 \times 10^{+3}$	$3.58 \times 10^{+4}$	$1.28 \times 10^{+5}$
17	$3.47 \times 10^{+3}$	$1.71 \times 10^{+11}$	0.93	$1.14 \times 10^{+4}$	$8.11 \times 10^{+4}$	$2.76 \times 10^{+5}$
18	$1.75 \times 10^{+3}$	$1.25 \times 10^{+11}$	0.46	$2.40 \times 10^{+3}$	$1.71 \times 10^{+4}$	$2.38 \times 10^{+4}$
19	$4.67 \times 10^{+3}$	$3.30 \times 10^{+11}$	0.29	$1.11 \times 10^{+4}$	$7.94 \times 10^{+4}$	$3.14 \times 10^{+5}$
20	$4.48 \times 10^{+3}$	$2.85 \times 10^{+11}$	0.86	$1.73 \times 10^{+4}$	$1.23 \times 10^{+5}$	$4.90 \times 10^{+5}$
21	$1.42 \times 10^{+3}$	$1.14 \times 10^{+11}$	0.02	$2.22 \times 10^{+2}$	$1.58 \times 10^{+3}$	$2.10 \times 10^{+3}$
22	$3.63 \times 10^{+3}$	$2.50 \times 10^{+11}$	0.26	$5.85 \times 10^{+3}$	$4.17 \times 10^{+4}$	$1.32 \times 10^{+5}$
23	$2.10 \times 10^{+3}$	$5.72 \times 10^{+10}$	1	$5.29 \times 10^{+3}$	$3.77 \times 10^{+4}$	$7.70 \times 10^{+4}$
24	$2.27 \times 10^{+3}$	$6.85 \times 10^{+10}$	0.16	$9.47 \times 10^{+2}$	$6.76 \times 10^{+3}$	$1.45 \times 10^{+4}$
25	$2.20 \times 10^{+2}$	$2.28 \times 10^{+11}$	0.43	$3.50 \times 10^{+2}$	$2.50 \times 10^{+3}$	$4.58 \times 10^{+2}$
26	$3.92 \times 10^{+2}$	$7.99 \times 10^{+10}$	0.83	$4.16 \times 10^{+2}$	$2.97 \times 10^{+3}$	$1.13 \times 10^{+2}$
27	$1.59 \times 10^{+3}$	$2.73 \times 10^{+11}$	0.32	$2.24 \times 10^{+3}$	$1.59 \times 10^{+4}$	$3.37 \times 10^{+4}$
28	$5.00 \times 10^{+3}$	$2.05 \times 10^{+11}$	0.36	$1.39 \times 10^{+4}$	$9.90 \times 10^{+4}$	$4.05 \times 10^{+5}$
29	$1.93 \times 10^{+3}$	$1.82 \times 10^{+11}$	0.66	$4.09 \times 10^{+3}$	$2.92 \times 10^{+4}$	$3.85 \times 10^{+4}$
30	$4.32 \times 10^{+3}$	$4.58 \times 10^{+10}$	0.73	$1.36 \times 10^{+4}$	$9.68 \times 10^{+4}$	$3.64 \times 10^{+5}$

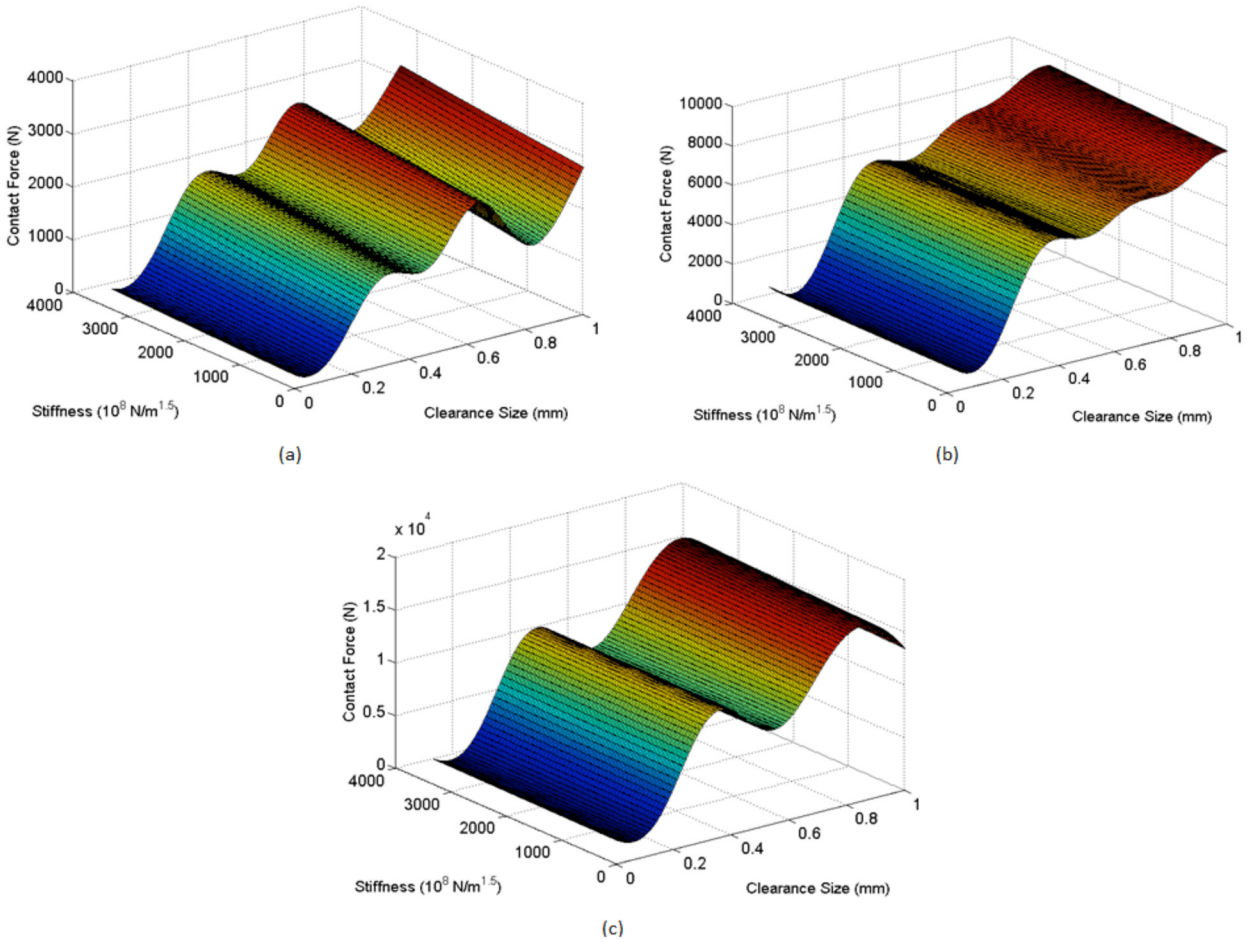

Fig. 16 Surface plots for contact forces: (*a*) low-speed input, (*b*) medium-speed input, and (*c*) high-speed input

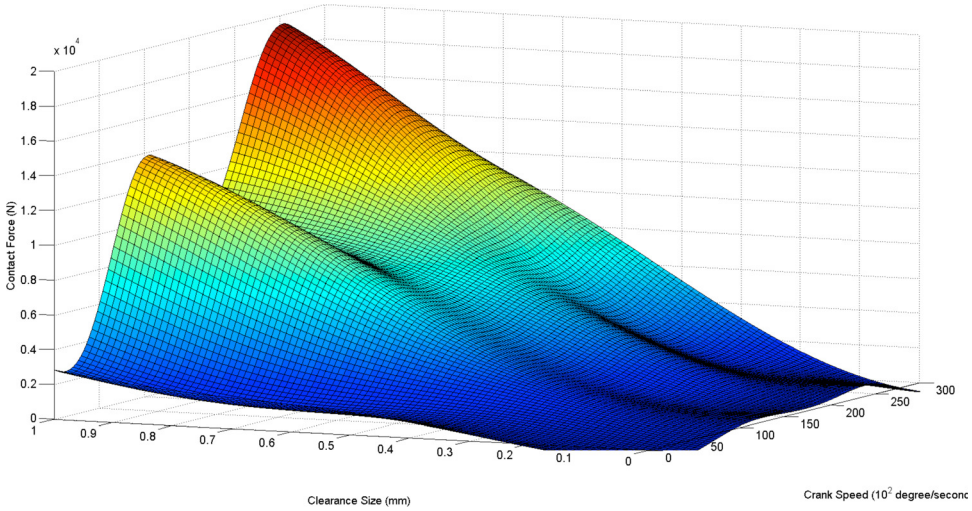

Fig. 17 Dynamic response in terms of contact force with constant stiffness coefficient

used to replace the computer simulation experiment. A similar accuracy test, as in the demonstrative example 1, is presented again for this example. After obtaining 30 design points by Latin hypercube sampling, another point (the 31st point) is obtained to evaluate the accuracy of the Kriging model. This 31st point is set with the clearance size of 0.5 mm, contact stiffness of 2.2 $N/m^{1.5}$, and input crank speed of 3000 rpm. The highest absolute value of the slider acceleration from the computer simulation model is $4.5 \times 10^{+4} m/s^2$. The highest absolute value of the slider acceleration from the Kriging model is $4.4 \times 10^{+4}$ m/s^2. The results indicate that the respective error for the highest absolute value of acceleration for the Kriging model is within 2% of the actual value. Hence, the Kriging model can reasonably predict the response of this system for the range of studied parameters.

Figure 16 shows the dynamic response histories of the contact forces between the bearing and the journal, as functions of the clearance size and the stiffness coefficient, with the input crank speed set to three different levels: the low-speed input of 1480 rpm, the medium-speed input of 3000 rpm, and the high-speed input of 4450 rpm. In each radial clearance situation, the contact force remains constant with respect to the stiffness coefficient, as shown in Fig. 16(*b*). However, the contact force between the bearing and the journal shows a clear increase for an increase in the clearance size. In this case, the effects of the dynamic response are more sensitive to the clearance size than the stiffness coefficient in this mechanical system with one revolute clearance joint. Figure 16 also indicates that when the mechanical system operates at the lower- and higher-speed levels, the nonperiodic behavior can clearly be observed. The curve for the contact force is more linear when the system operates at the medium-speed level. The contact force and the crank speed are positively correlated in this case. Similar conclusions can be drawn from Fig. 17, since it illustrates the influence of the radial clearance and crank speed on the contact force for a given stiffness coefficient of $1.63 \times 10^{+11}$ $N/m^{1.5}$. A rising trend of the contact force between the bearing and the journal is obtained with an increase in the radial clearance size and crank speed.

6 Conclusion

The influence of the dynamic behavior of a multibody mechanical system with a revolute clearance joint was investigated in this study. A computer-aided analysis of the mechanical system and the framework of the DOE modeling were presented to study the effect of the joint clearance size, input crank speed, and material/contact stiffness coefficient on the dynamic response of a multibody system with one clearance joint. The classical slider-crank mechanism with revolute joint clearance at the piston pin was considered in this study. The Kriging meta-model was used to replace the computer simulation experiment as a cost-effective mathematical tool for optimizing the system performance.

This research was focused on using the design-of-experiment method to develop a surrogate Kriging meta-model instead of the computer simulation model. The use of the Kriging model allowed the prediction of the system's response at other design points with a significantly lower computational time and cost. For the studied mechanism, the predictions were shown to be within 5% of the actual values from dynamic simulations, for which close to an hour of computational time is to be spent for each simulation. In addition to the use of the Kriging model for the prediction of the response at different design points, the scheme allows for the visualization of the trends of the response surfaces when the design variables are changed. The global results obtained from this study indicate that the dynamic behavior of the mechanical system with clearance is quite sensitive to the crank speed and clearance size. The contact force is increased when the crank speed increases and the decrease in crank speed tends to make the results more noisy. The contact force significantly increases with the increase in the clearance size and, as the clearance size decreases, the dynamic behavior tends to be close to the ideal situation. The dynamic response of the mechanism does not significantly change with a change in the contact stiffness coefficient. In general, the reduction in the input crank speed and clearance size minimizes the contact force between the bearing and the journal.

The method presented in this paper can be utilized for optimizing the performance of mechanical systems with joint clearances. By utilizing the Kriging meta-model, the computer simulation time can be significantly reduced, while the response of the system can be studied and optimized for a range of input design variables.

References

[1] Yuan, R. and Bai, G., 2009, "Comparison of Neural Network and Kriging Method for Creating Simulation-Optimization Metamodels," Proceedings of the Eighth IEEE International Conference, Dependable Autonomic and Secure Computing, DASC'09.

[2] Laribi, M. A., Mlika, A., Romdhane, L., and Zeghloul, S., 2004, "A Combined Genetic Algorithm-Fuzzy Logic Method (GA-FL) in Mechanisms Synthesis," Mech. Mach. Theory, **39**(7), pp. 717–735.

[3] Erkaya, S. and Uzmay, I., 2008, "A Neural-Genetic (NN-GA) Approach for Optimizing Mechanisms Having Joints With Clearance," Multibody Syst. Dyn., **20**(1), pp. 69–83.

[4] Flores, P. and Lankarani, H. M., 2012, "Dynamic Response of Multibody Systems With Multiple Clearance Joints," ASME J. Comput. Nonlinear Dyn., **7**(3), p. 031003.

[5] Flores, P., Ambrósio, J., Claro, J. C. P., and Lankarani, H. M., 2008, "Kinematics and Dynamics of Multibody Systems With Imperfect Joints:

Models and Case Studies," *Lecture Notes in Applied and Computational Mechanics*, Vol. 34, Springer-Verlag, New York.
[6] Haug, E. J. and Huston, R. L., 1985, "Computer Aided Analysis and Optimization of Mechanical System Dynamics," ASME J. Appl. Mech., **52**(1), pp. 243.
[7] Dubowsky, S., Norris, M., Aloni, E., and Tamir, A., 1984, "An Analytical and Experimental Study of the Prediction of Impacts in Planar Mechanical Systems With Clearances," ASME J. Mech., Transm., Autom. Des., **106**(4), pp. 444–451.
[8] Dubowsky, S. and Moening, M., 1978, "An Experimental and Analytical Study of Impact Forces in Elastic Mechanical Systems With Clearances," Mech. Mach. Theory, **13**(4), pp. 451–465.
[9] Furuhashi, T., Morita, N., and Matsuura, M., 1977, "Dynamic Researches of Four-Bar Linkage With Clearance at Turning Pairs: 4th Report, Forces Acting at Joints of Crank-Lever Mechanism," Trans. Jpn. Soc. Mech. Eng., **43**(376), pp. 4644–4651.
[10] Lankarani, H. M. and Nikravesh, P. E., 1990, "A Contact Force Model With Hysteresis Damping for Impact Analysis of Multibody Systems," ASME J. Mech. Des., **112**(3), pp. 369–376.
[11] Flores, P., Ambrosio, J., Claro, J. C. P., Lankarani, H. M., and Koshy, C., 2006, "A Study on Dynamics of Mechanical Systems Including Joints With Clearance and Lubrication," Mech. Mach. Theory, **41**(3), pp. 247–261.
[12] Flores, P., Lankarani, H. M., Ambrósio, J., and Claro, J. C. P., 2004, "Modelling Lubricated Revolute Joints in Multibody Mechanical Systems," Proc. Inst. Mech. Eng., Part K, **218**(4), pp. 183–190.
[13] Flores, P. and Lankarani, H. M., 2010, "Spatial Rigid-Multi-Body Systems With Lubricated Spherical Clearance Joints: Modeling and Simulation," Nonlinear Dyn., **60**(1–2), pp. 99–114.
[14] Mahrus, D., 1974, "Experimental Investigation Into Journal Bearing Performance," Rev. Bras. Tecnol., **5**(3–4), pp. 139–152.
[15] Wilson, R. and Fawcett, J. N., 1974, "Dynamics of Slider-Crank Mechanism With Clearance in the Sliding Bearing," Mech. Mach. Theory, **9**(1), p. 61–80.
[16] Haines, R. S., 1980, "A Theory of Contact Loss at Resolute Joints With Clearance," Proc. Inst. Mech. Eng., Part C: J. Mech. Eng. Sci., **22**(3), pp. 129–136.
[17] Flores, P., Ambrósio, J., Claro, J. C. P., and Lankarani, H. M., 2007, "Dynamic Behaviour of Planar Rigid Multi-Body Systems including Revolute Joints With Clearance," Proc. Inst. Mech. Eng., Part K, **221**(2), pp. 161–174.
[18] Bengisu, M. T., Midayetoglu, T., and Akay, A., 1986, "A Theoretical and Experimental Investigation of Contact Loss in the Clearances of a Four-Bar Mechanism," ASME J. Mech., Transm., Autom. Des., **108**, pp. 237–244.
[19] Feng, B., Morita, N., and Torii, T., 2002, "A New Optimization Method for Dynamic Design of Planar Linkage With Clearances at Joints—Optimizing the Mass Distribution of Links to Reduce the Change of Joint Forces," ASME J. Mech. Des., **124**(1), pp. 68–73.
[20] Tsai, M. and Lai, T., 2004, "Kinematic Sensitivity Analysis of Linkage With Joint Clearance Based on Transmission Quality," Mech. Mach. Theory, **39**(11), pp. 1189–1206.
[21] Yildirim, S., Erkaya, S., Su, S., and Uzmay, I., 2005, "Design of Neural Networks Model for Transmission Angle of a Modified Mechanism," J. Mech. Sci. Technol., **19**(10), pp. 1875–1884.
[22] Flores, P., Koshy, C. S., Lankarani, H. M., Ambrósio, J., and Claro, J. C. P., 2011, "Numerical and Experimental Investigation on Multibody Systems With Revolute Clearance Joints," Nonlinear Dyn., **65**(4), pp. 383–398.
[23] Hirsa, A., 2011, *Computational Methods in Finance*, CRC, Boca Raton, FL, pp. 224–228.
[24] Simpson, T. W., Mauery, T. M., Korte, J. J., and Mistree, F., 1998, "Comparison of Response Surface and Kriging Models for Multidisciplinary Design Optimization," Proceedings of the 7th AIAA/USAF/NASA/ISSMO Symposium on Multidisciplinary Analysis and Optimization, AIAA Paper No. 98–4758.
[25] Kbiob, D. G., 1951, "A Statistical Approach to Some Basic Mine Valuation Problems on the Witwatersrand," J. Chem. Metall. Min. Soc. S. Afr., **52**, pp. 119–139.
[26] Cressie, N., 1990, "The Origins of Kriging," Math. Geol., **22**(3), pp. 239–252.
[27] Forrester, A., Sobester, A., and Keane, A., 2008, *Engineering Design Via Surrogate Modeling: A Practical Guide*, Wiley, New York.
[28] Goldberg, D. E., 1985, *Genetic Algorithms in Search, Optimization, and Machine Learning*, Addison-Wesley, Reading, MA.
[29] Gear, C. W., Leimkuhler, B., and Gupta, G. K., 1985, "Automatic Integration of Euler-Lagrange Equations With Constraints," J. Comput. Appl. Math., **12**, pp. 77–90.
[30] Flores, P., Machado, M., Seabra, E., and Silva, M. T., 2011, "A Parametric Study on the Baumgarte Stabilization Method for Forward Dynamics of Constrained Multibody Systems," ASME J. Comput. Nonlinear Dyn., Vol **6**(1), p. 011019.